LARGE EDDY SIMULATION OF WOOD COMBUSTION

by

Simo Hostikka
VTT Building and Transport
Espoo, Finland
and
K.B. McGrattan
Building and Fire Research Laboratory
National Institute of Standards and Technology
Gaithersburg, MD 20899, USA

Reprinted from the Interscience Communications Ltd.; Building Research Establishment; National Fire Protection Association; National Institute of Standards and Technology; Society of Fire Protection Engineers; and Swedish National Testing and Research Institute. Interflam '2001. International Interflam Conference, 9th Proceedings. Volume 1. September 17-19, 2001, Edinburgh, Scotland, Interscience Communications Ltd., London, England, 755-762 pp, 2001.

LARGE EDDY SIMULATION OF WOOD COMBUSTION

Simo Hostikka
VTT Building and Transport
Espoo, Finland

Kevin McGrattan
NIST Building and Fire Research Laboratory
Gaithersburg MD, USA

The purpose of this work is to study the coupling of the one-dimensional pyrolysis model to the computational fluid dynamics model for the fire simulation. The large eddy simulation of the gas phase flow is combined with the combustion model using flame sheet approximation and a finite volume model for radiation. The model is used to predict the full-scale flame spread in a room with wood linings. The performance of the model is studied by comparing the predicted heat release rate, heat flux and surface temperatures with measurements.

INTRODUCTION

One of the ultimate goals of fire modeling is to predict flame spread and extinguishment over practical building materials and furnishings. In addition to individual solid and gas phase models, the coupling between the phases must be captured so that the burning rate is predicted rather than prescribed. Recent numerical studies[1] of the solid phase pyrolysis have used computational fluid dynamics (CFD) for the modeling of this coupling. These studies have shown that in small scale, where an external source of radiation is usually present, the effect of the flame feedback does not control or sustain the pyrolysis. However, at larger scales the flame feedback is likely to dominate the net heat flux, and correspondingly the overall burning rate. This presents a challenge to the fire model, which must capture the essential dynamics at different scales.

Using results from small-scale experiments, it is possible to validate the values used for the rate parameters of pyrolysis, the heat of vaporization, and the assumptions made in the modeling of the wood-substrate boundary condition. It is clear that the general applicability of the model is difficult to achieve, because the length scales of potential applications vary by several orders of magnitude. In the smallest scale, which usually means the simulation of laboratory experiments, the spatial accuracy may allow realistic prediction of the flame structure and temperature, thus approaching a direct numerical simulation of the flame. However, more practical applications range from room fires to industrial halls, and even forest fires. As the spatial discretization gets coarser, it becomes evident that the applied methods must be robust and simple, but still capable of simulating the essential dynamics.

In this work the pyrolysis model of Ritchie *et al*.[2] has been combined with the computational fluid dynamics code using large eddy simulation to predict the gas phase flow. The pyrolysis is modeled as an Arrhenius reaction converting virgin wood to char. The heat conduction and the development of the char layer are solved in one dimension. The radiative heat transfer is calculated with a fast finite volume method, which solves the radiative transport equation in a gray, non-scattering medium. Direction dependence of the radiation is captured by solving the equation in several directions, associated with small control angles. Gas phase combustion is modeled using the flame sheet approximation.

To exploit the generality of the model and selected parameters, a series of small scale experiments is simulated, and the results are compared. The capability of the model to predict full scale heat release rates is studied by simulating an experiment involving wood linings in the ISO 9705 room.

MODEL DESCRIPTION

Hydrodynamic model

The fluid flow is modeled by solving the conservation equations for mass, mixture fraction, momentum and energy in a low Mach number form[3,4]

$$\frac{\partial \rho}{\partial t} + \nabla \cdot \rho \mathbf{u} = 0 \tag{1}$$

$$\frac{\partial}{\partial t}(\rho Z) + \nabla \cdot \rho Z \mathbf{u} = \nabla \cdot \rho D \nabla Z \tag{2}$$

$$\rho\left(\frac{\partial \mathbf{u}}{\partial t} + \frac{1}{2}\nabla|\mathbf{u}|^2 - \mathbf{u} \times \omega\right) + \nabla \tilde{p} = (\rho - \rho_\infty)\mathbf{g} + \nabla \cdot \boldsymbol{\tau} \tag{3}$$

$$\rho c_p\left(\frac{\partial T}{\partial t} + \mathbf{u} \cdot \nabla T\right) = \dot{q}_C''' - \nabla \cdot \mathbf{q}_R + \nabla \cdot k \nabla T \tag{4}$$

where ρ, $\mathbf{u}$, Z and T are the density, velocity vector, mixture fraction and temperature. D is the diffusivity, $\tilde{p}$ the perturbation pressure, $\boldsymbol{\tau}$ the viscous stress tensor and k the thermal conductivity. $\dot{q}'''$ and $-\nabla \cdot \mathbf{q}_R$ are the source terms due to the chemical reactions and radiation, respectively. These equations are supplemented by an equation of state

$$p_0 = \rho R T \sum_i Y_i / M_i \tag{5}$$

where the pressure is replaced by an average pressure p_0 to filter out the acoustic waves. R is the ideal gas constant and Y_i and M_i are the species mass fractions and mole mass. p_0 is constant unless the domain is tightly sealed, in which case it depends only on time.

The most important approximation in the model is that the momentum equation can be simplified by substituting

$$\nabla H = \nabla\left(\frac{1}{2}|\mathbf{u}|^2 + \frac{\tilde{p}}{\rho}\right) \approx \frac{1}{2}\nabla|\mathbf{u}|^2 + \frac{1}{\rho}\nabla\tilde{p} \tag{6}$$

This approximation is equivalent to neglecting the baroclinic torque as a source of vorticity. The value of H is solved by taking the divergence of the momentum equation, using the equation of state and solving the resulting Poisson equation by a fast, direct method. The final form of the momentum equation is now

$$\frac{\partial \mathbf{u}}{\partial t} + \mathbf{u}\times\omega + \nabla H = \frac{1}{\rho}\left[(\rho - \rho_\infty)\mathbf{g} + \nabla\cdot\boldsymbol{\tau}\right] \tag{7}$$

The effect of the flow field turbulence is modeled using LES, in which the large scale eddies are computed directly and the sub-grid scale dissipative processes are modeled.

Combustion model

The combustion model is based on the assumption that the combustion is mixing-controlled. This implies that all species of interest can be described in terms of the mixture fraction Z, a conserved scalar variable. Heat from the reaction of fuel and oxygen is released along an infinitely thin sheet where Z takes on its stoichiometric value as determined by the solution of the transport equation for Z. The heat release rate per unit area of flame surface is

$$\dot{q}''_C = \Delta H_O \left.\frac{dY_O}{dZ}\right|_{z<z_f} (\rho D)\nabla Z\cdot\mathbf{n} \tag{8}$$

where ΔH_O is the energy released per unit mass of oxygen consumed[5] and $\mathbf{n}$ is the outward facing unit normal. Note that both dY_O/dZ and $\nabla Z\cdot\mathbf{n}$ are negative. ΔH_O should correspond to the amount of oxygen originating outside the fuel. The state relations are calculated for a stoichiometric reaction of $C_{3.4}H_{6.2}O_{2.5}$, that was previously used to model the combustion of Douglas fir[2] and the heat of combustion is assumed to be 12 MJ/kg, corresponding to ΔH_O = 9.26 MJ/kg(O_2).

Thermal radiation model

The Radiative Transport Equation (RTE) for a non-scattering gray gas is

$$\mathbf{s}\cdot\nabla I(\mathbf{x},\mathbf{s}) = \kappa(\mathbf{x})\left[I_b(\mathbf{x}) - I(\mathbf{x},\mathbf{s})\right] \tag{9}$$

where $I(\mathbf{x},\mathbf{s})$is the radiation intensity, $\mathbf{s}$ is the unit normal direction vector and the source term is due to the blackbody radiation $I_b = \sigma T^4/\pi$. The wall boundaries are assumed to be diffuse and gray. Absorption coefficient $\kappa(\mathbf{x})$ is calculated using RADCAL narrow-band model[6] and tabulated as a function of mixture fraction and temperature before the actual simulation. The radiative transport equation (11) is solved using the Finite Volume Method[7], a technique similar to those for convective transport for fluid flow. The discretized form of the RTE is obtained by dividing the solid angle into a finite number of control angles, as shown in Figure 1. Equation (11) is then integrated over the cell volume V_{ijk} and the control angle $\delta\Omega_l$. Volume integrals are transformed to sums over the cell faces by assuming that the radiation

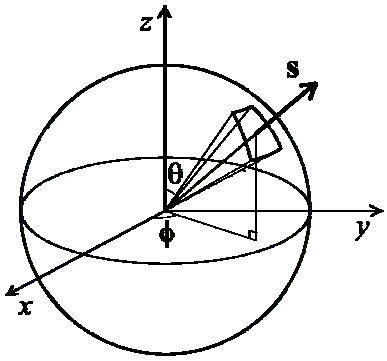

Figure 1. The coordinate system of the angular discretization.

intensity is constant on the cell boundaries, within the cell volume and over the angle $\delta\Omega_l$. On a Cartesian grid system the resulting system can be solved very efficiently using an explicit marching sequence[8]. The intensities on the cell boundaries are calculated using a first order upwind method, and the integrals over the control angles are calculated analytically before the actual simulated. The radiation solver is called every third time step of the flow solver, and on each call, only every fifth angle is updated. As a result, it takes 15 time steps to update all the control angles.

Solid-phase model

The heat transfer and pyrolysis inside the wood material are modeled using the one-dimensional model of Atreya[9], which was further developed by Ritchie *et al.*[1]. The model is applied on each wood material surface cell of the computational domain. It describes the evaporation of moisture and the degradation of the virgin wood to gaseous fuel and char. The volatile gases are instantaneously released to the gas space. The governing equation for energy is

$$\overline{\rho c}\frac{\partial T}{\partial t}=\frac{\partial}{\partial x}\left(\lambda_w\frac{\partial T}{\partial x}\right)+\frac{\partial \rho_w}{\partial t}\left[\Delta H_{py}-C\left(T-T_0\right)\right]+\frac{\partial \rho_m}{\partial t}\left[\Delta H_{ev}-D\left(T-T_0\right)\right] \tag{10}$$

where ρ_w is the total density of wood and ρ_m is the moisture density. ΔH_{py} and ΔH_{ev} are the heat of pyrolysis and the heat of water evaporation. Coefficient C and D are defined as

$$C=\frac{\rho_{w0}\overline{c_{p,w0}}-\rho_{wf}\overline{c_{p,wf}}}{\rho_{w0}-\rho_{wf}}-\overline{c_{p,g}} \tag{11}$$

$$D=\overline{c_{p,m}}-\overline{c_{p,g}} \tag{12}$$

where ρ_{w0}, $c_{p,w0}$, ρ_{wf} and $c_{p,wf}$ are the densities and specific heats of virgin wood and char, respectively, and $c_{p,g}$ and $c_{p,m}$ are the specific heats of gaseous products and moisture. The overbars in Equations (11) and (12) denote evaluation at the average of instantaneous temperature T and initial temperature T_0. The pyrolysis rate is modeled as a first order Arrhenius reaction

$$\frac{\partial \rho_w}{\partial t} = -\rho_a A e^{-E_A/RT} \tag{13}$$

where ρ_a is the density of active wood, A is the pre-exponential factor and E_A is the activation energy. The evaporation of moisture is assumed to consume all the available energy, once the material has reached an evaporation temperature T_{ev}

$$\frac{\partial \rho_m}{\partial t} = -\frac{\partial}{\partial x}\left(\lambda_w \frac{\partial T}{\partial x}\right)\left[\Delta H_{ev} - D(T - T_0)\right]^{-1}\Bigg|_{T=T_{ev}} \tag{14}$$

The following definitions are used to calculate the thermal properties of the wood during the drying and charring processes.

$$\overline{\rho c} = \left(\rho_a c_{p,w0} + \rho_c c_{p,wf} + \rho_m c_{p,m}\right) \qquad \lambda_w = \lambda_{w0}\left(\frac{\rho_a}{\rho_{w0}}\right) + \lambda_{wf}\left(\frac{\rho_c}{\rho_{wf}}\right) \tag{15}$$

$$\rho_a = \rho_{w0}\frac{\rho_w - \rho_{wf}}{\rho_{w0} - \rho_{wf}} \qquad \rho_c = \rho_w - \rho_a$$

where the thermal properties of virgin wood and char, $c_{p,w0}$, $c_{p,wf}$, λ_{w0} and λ_{wf}, depend on the local temperature T, as shown in Table 1. Similar equations are applied to be substrate as well, with pyrolysis and evaporation terms set to zero. The boundary conditions are defined by the gas phase models of the CFD-code.

Table 1. Parameters of the solid phase model.

	Variable	Value	Ref.
A	pre-exponential factor	$1.5 \cdot 10^2$ s^{-1}	best fit
α_{subs}	substrate thermal diffusivity	$6.1 \cdot 10^{-7}$ m^2/s	1
$c_{p,g}$	specific heat of volatiles	$5.24{\cdot}10^{-1} + 1.84{\cdot}10^{-3}\ T - 3.76{\cdot}10^{-7}\ T^2$ kJ/kg·K	11
$c_{p,m}$	specific heat of moisture	4.19 kJ/kg·K	
$c_{p,wf}$	specific heat of char	$-1.47 + 1.14{\cdot}10^{-2}\ T - 1.65{\cdot}10^{-5}\ T^2 + 1.09{\cdot}10^{-8}\ T^3 - 2.66{\cdot}10^{-12}\ T^4$ kJ/kg·K	10
$c_{p,w0}$	specific heat of virgin wood	$0.10 + 0.0037\ T$ kJ/kg·K	10
ΔH_{ev}	heat of evaporation	2260.0 kJ/kg	
ΔH_{py}	heat of pyrolysis	125.6 kJ/kg	1
ε	surface emissivity	0.8 … 1.0	10
E_A	activation energy	$0.5 \cdot 10^5$ kJ/kmol	best fit
λ_{subs}	substrate conductivity	$0.03{\cdot}10^{-3}$ kW/m·K	best fit
λ_{wf}	char conductivity	$4.88{\cdot}10^{-5} + 9.46{\cdot}10^{-8}$ kW/m·K	1
λ_{w0}	virgin wood conductivity	$0.03{\cdot}10^{-3} + 3.3{\cdot}10^{-7}$ kW/m·K	11
ρ_m	moisture density	46.2 kg/m^3	13
ρ_{wf}	char density	120.0 kg/m^3	11
ρ_{w0}	dry virgin wood density	393.8 kg/m^3	13

The selection of the proper material properties and the pyrolysis rate coefficients is a very difficult task. Most of the thermal properties must be taken from the previous works[2,10,11] but the applicability of that data to the current spruce wood is not guaranteed. The biggest

uncertainty is related to the coefficients of the pyrolysis model, as the values derived from small and large scale experiments may have a several orders of magnitude difference[9]. Some of the values found in literature are summarized in Table 2. The values used in this work were found fitting the numerical results to the measurements.

Table 2. Literature values for the pyrolysis rate coefficients.

Source	Wood type	A (s^{-1})	E_A (kJ/kmol)
Parker[10]	Douglas Fir	2.5×10^8	1.26×10^5
Novozhilov *et al.*[1]	particle board	5.25×10^7	1.256×10^5
Atryea[9]	pine, spruce and fir woods	5.1×10^{11}	1.26×10^5
Fredlund[11]	spruce	0.54	0.263×10^5
DiBlasi[12]	lignocellulosic material,	1) 2.8×10^{19}	2.42×10^5
	3-step mechanism	2) 1.3×10^{10}	1.51×10^5
		3) 3.3×10^4	1.97×10^5

RESULTS AND DISCUSSION

Pyrolysis in the cone calorimeter

The performance of the pyrolysis model was tested by modeling the cone calorimeter tests conducted at four different radiation levels[13]. For this purpose the pyrolysis model was separated from the CFD-code and the flame convection and radiation were calculated using simple correlations, following the example of ref. 1. Calculated and measured heat release rates are compared in Figure 2. As can be seen, the selected rate parameters give good results for the 50 and 30 kW/m^2 radiation levels, but too fast ignition is achieved for the smaller heat fluxes. It should be noted, that the burning rates at small radiation levels are usually much more difficult to predict, as the errors in the heat transfer solution and thermal properties become more important. The absence of some physical phenomena, like surface reactions and internal mass transfer, may also affect the results at small radiation levels.

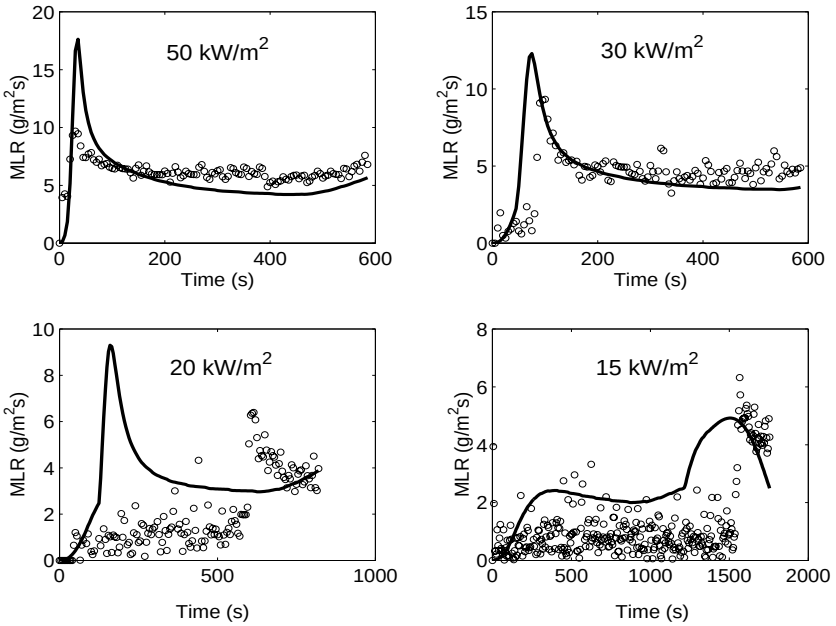

Figure 2. Comparison of the measured (circles) and predicted (continuous line) mass loss rates in cone calorimeter experiments.

Room scale flame spread

The CFD model was used to predict the heat release rate and fire environment conditions in a full scale fire test, conducted at VTT Building and Transport[13]. The experimental scenario is shown in Figure 3. One third of the room surface area was covered by 22 mm spruce panels. The walls and ceiling were light weight concrete and the floor was normal concrete. The fire was ignited using a 100 kW propane burner in the corner. The total heat release rate was measured using oxygen consumption calorimetry. Additional measurements included the total heat flux in the middle of the floor and the wall surface temperatures in five vertical locations at 1.0 m horizontal distance from the corner.

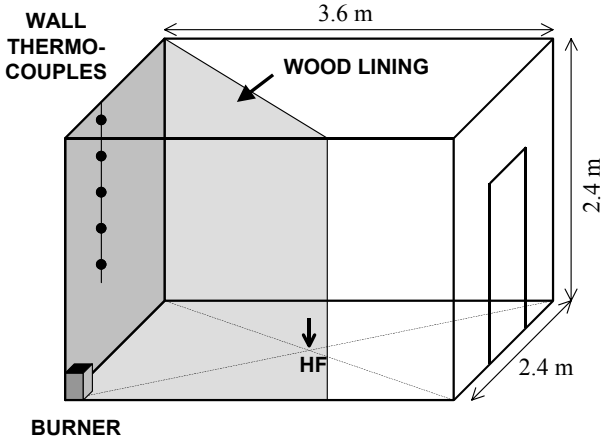

Figure 3. Geometry and measurement points of the flame spread experiment [13].

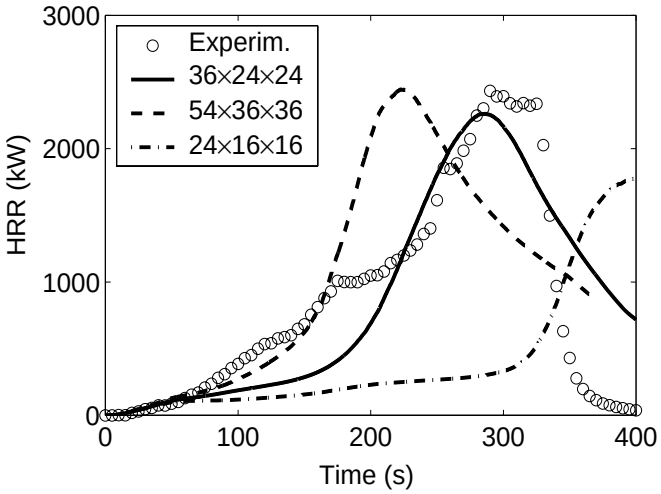

Figure 4. Comparison the measured and predicted heat release rates with different computational grids. 36×24×24 was used through the rest of this work.

A non-uniform cartesian grid was used with 36 × 24 × 24 cells in *x*, *y* and *z*-directions. The effect of the grid dimension was studied, and will be reported below. The door was described as an open boundary, and one dimensional heat transfer boundary conditions with appropriate thermal properties were applied on the room boundaries. One simulation took approximately 9 h on a 700 MHz PC.

Figure 4 shows a comparison of the measured and predicted heat release rates. The results are shown for three different grids. Strong grid dependence can be seen in the HRR curves, which is probably due to the effect of the cell size on the flame temperatures near the flame front. It is practically impossible to solve the convective heat transfer between the flame front and wall using the cell size of few centimeters. This is clearly seen during the first 150 s of the fire, when the increase of the HRR is mainly due to the upward and horizontal flame spread. After 150 s the flame spread is controlled by radiation, as the lower part of the walls are ignited. One of the challenges in the full scale flame spread modeling is that a good quantitative agreement during the first phase may be required to reach good qualitative results later on. Another challenge, caused by the gap between the resolved scales and the scales of the pyrolysis front, is that the rate coefficients derived from the small scale experiments do not give good results in large scale calculation. Instead, some kind of "effective" values must be used. Unfortunately, these values can only be adjusted using the numerical experiments in the scale of the actual application.

A comparison of the measured and predicted total heat fluxes in the middle of the floor is shown in Figure 5. The difference in the heat fluxes is caused by the corresponding difference in the heat release rates. Taking this into account and knowing that the prediction of the radiative heat fluxes is difficult in general, due to the strong dependence of the predicted temperature field, the agreement of the heat fluxes can be considered good.

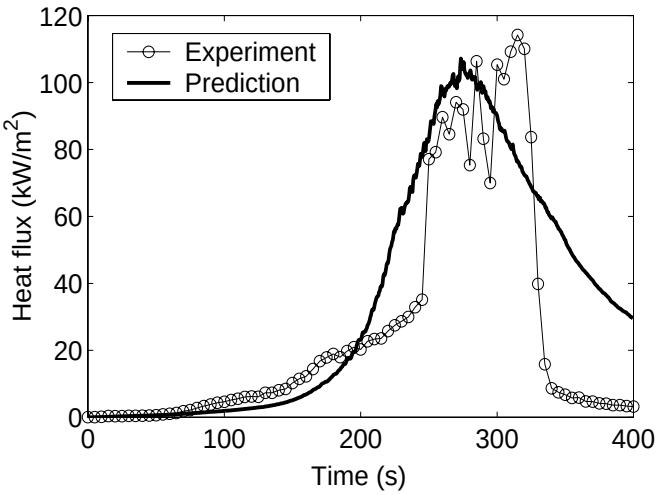

Figure 5. Comparison of the measured and predicted heat fluxes in the middle of the floor.

The measured and predicted wall surface temperatures are compared in Figure 6. Although the general agreement looks reasonable, some observations should be made: First, the heating of the highest thermocouple (15 cm below the ceiling) is slower than measured, indicating that the convective heat transfer or temperature is underpredicted. Secondly, the peak temperatures do not level off at 800 °C, which is typical for charring materials. This may be due to the underpredicted radiative emissions in the gas phase, causing too high gas temperatures in the smoke layer.

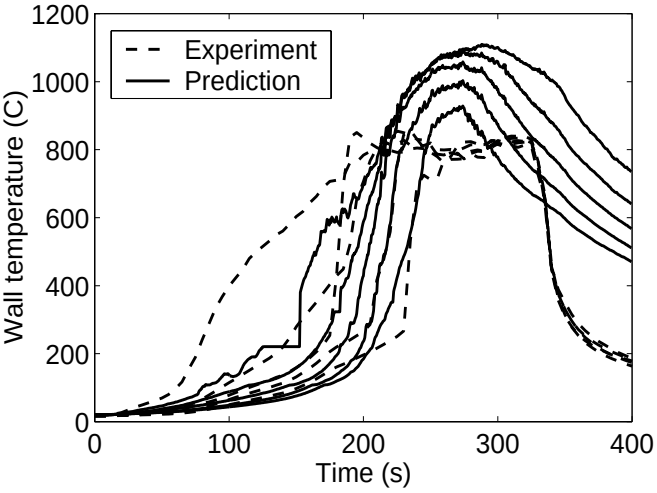

Figure 6. Comparison of the measured and predicted wall surface temperatures.

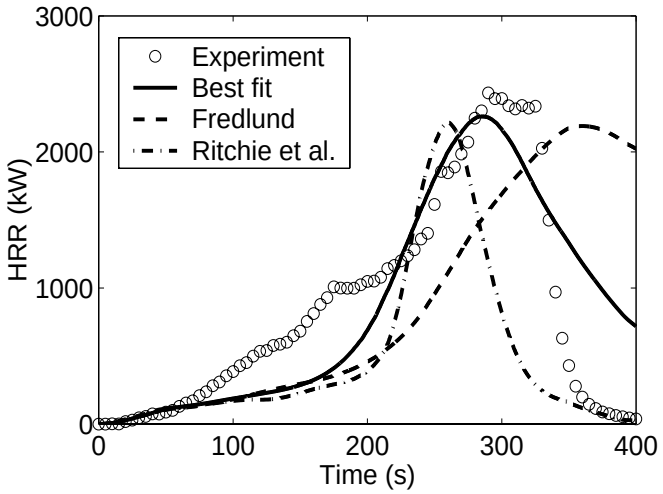

Figure 7. Effect of the pyrolysis rate coefficients on the predicted heat release rate.

The effect of the pyrolysis rate coefficients is demonstrated in Figure 7 where the measured heat release rate is compared with the prediction using different rate coefficients. Best fit values used in this work are $A = 1.5\times10^2$ s^{-1}, E_A=0.5×10^5 kJ/kmol. These values can be considered compromise between the small and large scale values. Fredlund's values[11] were A = 0.54 s^{-1} and E_A=0.263×10^5 kJ/kmol and Ritchie *et al.* [1] used $A = 2.5\times10^8$ s^{-1}, E_A=1.26×10^5 kJ/kmol. An additional difference between the simulations was the assumed chemical fuel composition: In the simulation using Fredlund's values the fuel was assumed to be $CH_{3.584}O_{1.55}$ and ΔH_c = 15 MJ/kg, while $C_{3.4}H_{6.2}O_{2.5}$ and ΔH_c = 12 MJ/kg were used elsewhere. General behavior of all the curves looks good, but none of the coefficient pairs produced the same kind of smooth increase as found in the measured curve. However, this may be mainly due to the heat transfer problems.

CONCLUSIONS

The large eddy simulations of the fires involving wood pyrolysis were conducted using mixture fraction based combustion model and finite volume model for radiation. The pyrolysis model was first applied to the small scale experiments. The agreement of the ignition times and burning rates was found to be good at high radiation levels, but larger errors were found at smaller levels. Flame spread experiment in the full scale room was used as primary application. The results were found to be grid dependent, mainly due to the unresolved scales near the flame front. More attention should be paid to the physical and numerical methods to resolve the flame boundary layers. However, the general agreement with the measured heat release rate and heat flux was found quite easily. A reasonable quantitative agreement was then reached by tuning the pyrolysis rate coefficients. Further improvement would be possible but hardly justified because the experimental uncertainty of a single test is not known, and because the number of poorly known parameters is so large.

ACKNOWLEDGEMENTS

The authors wish to thank Dr. Jukka Hietaniemi and Ms. Tuula Hakkarainen from VTT Building and Transport for providing the experimental data.

REFERENCE LIST

1. V. Novozhilov, B. Moghtaderi, D.F. Fletcher and J.H.Kent. Computational Fluid Dynamics Modelling of Wood Combustion. *Fire Safety Journal*, 27: 69-84. 1996.

2. Ritchie, S.J.; Steckler, K.D.; Hamins, A.; Cleary, T.G.; Yang, J.C.; Kashiwagi, T. Effect of Sample Size on the Heat Release Rate of Charring Materials. Hasemi, Y. (ed.) Fifth (5th) International Symposium Fire Safety Science, pp. 177-188, 1997.

3. K.B. McGrattan, H.R. Baum, and R.G. Rehm. Large Eddy Simulations of Smoke Movement. *Fire Safety Journal*, 30:161–178, 1998.

4. R.G. Rehm and H.R. Baum. The Equations of Motion for Thermally Driven, Buoyant Flows. *Journal of Research of the NBS*, 83:297–308, 1978.

5. J.E. Floyd, H.R. Baum, and K.B. McGrattan. A Mixture Fraction Combustion Model for Fire Simulation Using CFD. Proceedings of the International Conference on Engineered Fire Protection Design, Societey of Fire Protection Engineers. pp. 279-290. 2001.

6. W.L. Grosshandler. RADCAL: A Narrow-Band Model for Radiation Calculations in a Combustion Environment. National Institute of Standards and Technology. NIST Technical Note 1402. 1993.

7. G.D. Raithby and E.H. Chui. A Finite-Volume Method for Predicting Radiant Heat Transfer in Enclosures with Participating Media. *Journal of Heat Transfer*, 112(2):415–423, 1990.

8. S.H. Kim and K.Y. Huh. Assessment of The Finite-Volume Method and The Discrete Ordinate Method for Radiative Heat Transfer In a Three-Dimensional Rectangular Enclosure. *Numerical Heat Transfer, Part* B, 35:85–112, 1999.

9. A. Atreya. Pyrolysis, Ignition and Fire Spread on Horizontal Surfaces of Wood. National Bureau of Standards. Report NBS-GCR-83-449. 1984.

10. W.J. Parker. Prediction of the Heat Release Rate of Douglas Fir. Proceedings of the 2nd Int. Symp. on Fire Safety Science. 337-346. 1989.

11. B. Fredlund. A Model for Heat and Mass Transfer in Timber Structures During Fire, A theoretical, numerical and experimental study. Report LUTVDG(TVBB-1003), Department of Fire Safety Engineering, Lund University, Sweden. 1988.

12. C. Di Blasi. Physico-chemical processes occuring inside a degrading two-dimensional anisontropic porous medium. *International Journal of of Heat and Mass Transfer*. 41:4139-4150, 1998.

13. J. Hietaniemi, T. Hakkarainen, E. Mikkola, M. Salonvaara, A. Nurmi and L. Vanhatalo. Wood Products with Improved Fire Performance. VTT Research Notes. To be published in 2001.